Physical and Biological Characteristics of the Antitumor Drug Actinomycin D Analogues Derivatized at *N*-Methyl-L-valine Residues[†]

Fusao Takusagawa,* Li Wen, Wenhua Chu, Qifang Li, Ken T. Takusagawa, Robert G. Carlson, and Robert F. Weaver

Department of Biochemistry, University of Kansas, Lawrence, Kansas 66045

Received April 8, 1996; Revised Manuscript Received June 26, 1996[⊗]

ABSTRACT: The crystal structure of the DNA-actinomycin D (AMD) complex and a simple molecular modeling study indicated that AMD analogues derivatized at *N*-methyl-L-valine residues (fifth amino acid residue in the cyclic depsipeptide of AMD) could bind to DNA as strongly as the parent AMD. The analogues in which *N*-methyl-L-valine residues were replaced with L- and D-forms of *N*-methylvalines, *N*-methylthreonines, *N*-methylphenylalanines, *N*-methyltyrosines, and *N*-methyl-*O*-methyltyrosines have been totally synthesized. The characteristics of binding of the analogues to various DNAs including DNA-1 [d(TATATATGCATATATA)], DNA-2 [d(TATATACGCGTATATA)], DNA-3 [d(ATATAT-AGCTATATAT)], and DNA-4 [d(ATATATGGCCATATAT)] have been examined by using visible absorption spectrum methods. The association constants calculated from the absorption spectra indicate that the modifications of the *N*-methyl-L-valine residues in the AMD molecule do affect the DNA binding characteristics of the analogues. The L-aromatic analogues bind slightly better than the L-aliphatic analogues except for binding to DNA-1 (-TGCA-), whereas the D-aliphatic analogues bind consistently better than the D-aromatic analogues. In the L-form analogues, the L-Tyr analogue has the highest overall association constant, whereas the D-Val analogue has the highest association constant among the D-form analogues. In spite of substitution of bulky aromatic groups, the D-aromatic analogues bind to the DNA-1 quite well. However, D-aromatic analogues have significantly reduced their binding capacities to the other DNAs, indicating that the substitution of the D-aromatic residues creates a unique four-base sequence preference (-TGCA-). The RNA polymerase inhibitory activities of the AMD analogues *in vivo* have been examined using human cells (HeLa). All AMD analogues except for the L-Thr analogues severely inhibit RNA synthesis at relatively low drug concentrations. The D-Val, L-OMT, L-Phe, and D-Phe analogues inhibit RNA synthesis more strongly than the natural antibiotic (AMD itself).

Many naturally occurring antibiotics contain cyclic depsipeptides closed by an ester linkage. Some of these act by binding to DNA. The planar residue (chromophore) intercalates between the base pairs of DNA, and the other moiety binds to the surface of double-helical DNA. The role of the planar residue is relatively well established, and it is also known that some amino acid residues in the depsipeptide ring are essential to bind the antibiotic to DNA by forming hydrogen bonds. However, although it is well recognized that the other amino acid residues are equally necessary to maintain the biological activity, the exact role of these residues is not well established. Thus, for example, it is extremely difficult to predict *a priori* precisely which chemical modification would be appropriate in order to increase the biological activity of the antibiotics isolated from nature.

Actinomycin D (AMD),[1] whose molecular formula is shown in Figure 1, contains a planar phenoxazone ring as well as two cyclic depsipeptide rings composed of five amino acid residues (Thr, D-Val, Pro, Sar, *N*-Me-Val) and is best known for its effectiveness as an inhibitor of transcription (Goldberg *et al.*, 1971; Kersten *et al.*, 1974; Waring, 1981). It has been employed clinically as an antitumor agent for treatment of highly malignant tumors such as Wilms tumor (Farber, 1966) and gestational choriocarcinoma (Lewis, 1972; Schink *et al.*, 1992). However, its selective toxicity is poor because it is an extremely potent, specific inhibitor of DNA-directed RNA synthesis in practically all types of cells which have been examined [reviewed by Meienhofer and Atherton (1977)]. Currently AMD is used with combinations of other antitumor drugs to treat high-risk tumors. For example, the EMA/CV regimen (etoposide, methotrexate, AMD, cyclophosphamide, vincristine) has been used to treat gestational trophoblastic tumors (Newlands *et al.*, 1991), and the VAC regimen (vincristine, AMD, cyclophosphamide) (Marina *et al.*, 1992) and the VAB-6 regimen (vinblastine, AMD,

[†] Research supported by NIH (AI28578), Marion Merrell Dow Foundation, J. R. and Inez W. Jay Research Foundation, and Kansas Health Foundation, Wichita, Kansas. The Kansas Health Foundation is an independent, non-profit organization whose mission is to improve the quality of health in Kansas.

* Author to whom correspondence should be addressed.

[⊗] Abstract published in *Advance ACS Abstracts,* September 15, 1996.

[1] Abbreviations: AMD, actinomycin D; L-Val-AMD, 5,5′-*N*-methyl-L-valine-AMD; D-Val-AMD, 5,5′-*N*-methyl-D-valine-AMD; L-Thr-AMD, 5,5′-*N*-methyl-L-threonineactinomycin D; D-Thr-AMD, 5,5′-*N*-methyl-D-threonineactinomycin D; L-Phe-AMD, 5,5′-*N*-methyl-L-phenylalanineactinomycin D; D-Phe-AMD, 5,5′-*N*-methyl-D-phenylalanine-actinomycin D; L-Tyr-AMD, 5,5′-*N*-methyl-L-tyrosineactinomycin D; D-Tyr-AMD, 5,5′-*N*-methyl-L-tyrosine-actinomycin D; L-OMT-AMD, 5,5′-*N*-methyl-L-*O*-methyltyrosineactinomycin D; D-OMT-AMD, 5,5′-*N*-methyl-L-*O*-methyltyrosineactinomycin D.

S0006-2960(96)00828-8 CCC: $12.00 © 1996 American Chemical Society

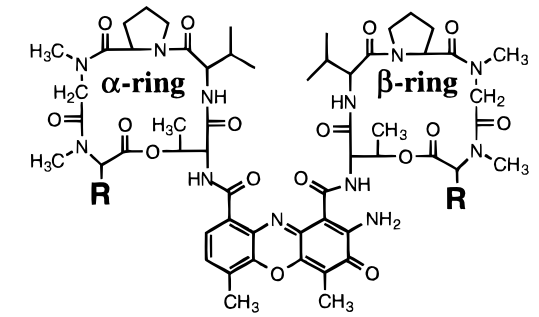

R	L-form	D-form
	L-Val-AMD	D-Val-AMD
	L-Thr-AMD	D-Thr-AMD
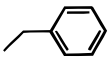	L-Phe-AMD	D-Phe-AMD
	L-Tyr-AMD	D-Tyr-AMD
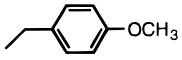	L-OMT-AMD	D-OMT-AMD

FIGURE 1: Molecular formulas of AMD and AMD analogues.

bleomycin) (Nakamura *et al.*, 1992) are used to treat childhood germ cell tumors.

Analogues of AMD have been produced by directed biosynthesis, partial synthesis, and total synthesis [reviewed by Meienhofer and Atherton (1977) and Mauger (1980, 1990)], in order to reduce its cytotoxicity while retaining most of its antitumor activity. In many cases, replacements of amino acid residues in the cyclic depsipeptides of AMD have been found to render such analogues inactive or less active. However, a few analogues have shown very promising results. For example, 5,5′-*N*-methylleucine-AMD (*N*-methylvaline at the C-terminal is replaced with *N*-methylleucine) displays less antimicrobial activity but higher antitumor activity than AMD itself *in vitro* (Mauger *et al.*, 1991). Recently, we have determined the crystal structures of the complexes between $d(GAAGCTTC)_2$ and AMD/N8-AMD (Kamitori & Takusagawa, 1992, 1994; Shinomiya *et al.*, 1995), in which AMD intercalated between the middle 5′-GC-3′ base pairs. These crystal structures of the complexes show how the drug interacts with DNA. In the DNA−AMD complex structures, the isopropyl groups of the D-valine residues are pointed to the outside of the complex, and thus these groups are considered not to participate in interaction with DNA. Therefore, AMD analogues in which the D-valine residues are replaced with other D-amino acid residues are expected to bind to DNA as strongly as AMD does. If AMD inhibits RNA synthesis by just binding intercalatively to DNA, these AMD analogues will inhibit RNA synthesis as strongly as AMD does. However, if the cyclic depsipeptides of AMD play an unexpected role in inhibition of RNA synthesis, replacement of the D-valine residues with other residues would affect the inhibition activities of the AMD analogues (Takusagawa, 1985). We have synthesized several AMD analogues with the D-valine replaced with aromatic D-amino acid residues and examined the effects of these replacements on DNA-binding characteristics and transcription inhibitory activities (Chu *et al.*, 1994). In this study, the D-valine residue has been found to be an important biological modulator of the antibiotic.

In addition to its biological importance, AMD has been studied as a model for drugs that bind to DNA sequence-specifically. Müller and Crothers (1968) investigated the binding properties of AMD analogues by hydrodynamic, kinetic, and thermodynamic studies. They have shown that drugs bind preferentially in the 5′-GC-3′ steps of double-stranded DNA by intercalation. The 5′-GC-3′ binding preference was confirmed by X-ray crystallography (Sobell *et al.*, 1971; Takusagawa *et al.*, 1982) and 2D-NMR studies (Brown *et al.*, 1984; Zhou *et al.*,1989; Liu *et al.*, 1991). Several thermodynamic investigations have established that enthalpies of AMD binding to DNA provide small negative values compared with other intercalators such as ethidium bromide and daunomycin, which bind to DNA with large enthalpic driving forces (Snyder *et al.*, 1989; Bailey *et al.*, 1993; Gellert *et al.*, 1965; Chou *et al.*, 1987; Breslauer *et al.*, 1987; Chen, 1988). It has been proposed that AMD binding occurs with a very large entropic driving force resulting from changes of hydrations around DNA (Gellert *et al.*, 1965; Marky *et al.*, 1983). This characteristic of the thermodynamic behavior of AMD may relate to the unusual solubility of AMD in water, which exhibits a large negative temperature dependence (Gellert *et al.*, 1965). Recently, it has been revealed by various biological analyses, *i.e.*, footprinting and transcription assays, that neighboring and next-neighboring bases of the 5′-GC-3′ steps affect the binding of AMD to DNA (Scamrov *et al.*, 1983; Goodismen *et al.*, 1992; Phillips *et al.*, 1986). Further, Chen studied the DNA binding affinity of AMD using a series of oligonucleotides containing different XGCY sites (Chen, 1988, 1992). He has reported that AMD binding strength decreases in the order of TGCA > CGCG > AGCT ≫ GGCC.

Here we report the syntheses of ten AMD analogues derivatized at the *N*-methyl-L-valine residues, and their DNA binding characteristics and RNA synthesis inhibitory activities.

EXPERIMENTAL PROCEDURES

Syntheses

Melting points are uncorrected. The NMR spectra were obtained with 300 MHz Varian XL-300 NMR Spectrometer. For the mass spectrum measurements, electron ionization (EI) and chemical ionization (CI) spectra were obtained on a Nermag R10-10 quadrupole GC/MS system with SPECTRAL 30 data system. Fast-atom bombardment mass spectra (FABMS) were obtained on a ZAB HS mass spectrometer. All mass spectrum measurements have been carried out at the Mass Spectrometry Laboratory of the University of Kansas. The homogeneity of the products was checked by thin-layer chromatography on silica-gel plates. The intermediates and the final products of the AMD analogues were confirmed by NMR and mass analyses. The details of syntheses of the AMD analogues are given in the supporting information.

DNA Syntheses

The self-complementary 16-mer DNAs, in which the AMD binding site (-GC-) is in the middle of the sequence, were

synthesized at 15 μM scale by a Cruachem PS-250 DNA/RNA synthesizer using the protocol provided from the company. After the deprotection procedure, the crude oligonucleotides were purified by reverse-phase HPLC using a C_{18} column.

UV/Vis Spectrum Measurements

UV/vis absorption spectra were measured on a JASCO V-560 double-beam spectrometer. All measurements were carried out at 2 °C in order to prevent DNA melting. The cuvette chamber was slightly modified to fill with −100 °C dew-point dry air to prevent the condensation of moisture on the cuvette windows. Stock solutions (20 μM of double-strand DNA) of the five DNAs were prepared with binding buffer (50 mM Tris-HCl, pH 7.5, 10 mM $MgCl_2$, and 10 mM KCl). All binding experiments were carried out in the same buffer. The concentrations of the five DNAs (single-strand) were determined from the absorbance at 260 nm using the extinction coefficients 17.15×10^4, 16.61×10^4, 16.77×10^4, 16.81×10^4, and 17.81×10^4 M^{-1} cm^{-1} (Cantor & Warshaw, 1970), respectively. The concentrations of AMD analogue solutions were determined from the absorbances at 440 nm using an extinction coefficient of 2.45×10^4 M^{-1} cm^{-1} (Chen, 1988).

The absorption spectra of drugs during titration with DNAs were stored on a computer disk to examine the binding characteristics of drugs to the DNAs. After the absorbance of 1.0 mL of drug solution (~1.0 μM) in binding buffer was measured from 600 to 350 nm at 2 °C, a small aliquot of a known concentration of the DNA solution was placed in the sample cuvette and spectra were measured ten minutes later. This procedure was repeated six times so that six spectra were measured at six different DNA concentrations. The absorbances of visible spectra were read at one nm intervals. Dilution factors were applied to all spectra. The base lines of the spectra of AMD analogues were slightly corrected with a straight line addition/subtraction, in order to superimpose the spectra on the AMD spectrum. The association constants of AMD analogues were calculated based on the spectra using the method developed in our laboratory (Chu *et al.*, 1994).

DNA Melting Profile Measurements

A JASCO HMC-358 constant temperature cell holder connected with a NESLAB RTE-111 bath circulator was used to obtain the melting profiles of DNA. A 10 μL aliquot of DNA solution (20 μM) was added into the sample cuvette containing 990 μL of binding buffer, and the absorption at 260 nm was measured from 0 to 65 °C. The cuvette temperature was monitored by putting a thermocouple directly in the cuvette; it increased approximately 0.5 degree per minute.

Water Solubility Measurements

AMD and AMD analogues were dissolved in the binding buffer until the compounds were saturated. After centrifugation, the concentrations of drugs were determined spectrophotometrically.

RNA Polymerase Inhibition

Human (HeLa) cells were cultured at 37 °C in a 1:1 mixture of DME and Harn's F-12 medium, supplemented with penicillin and streptomycin and 5% fetal bovine serum, in an atmosphere of 5.5% CO_2, using a total sodium bicarbonate concentration of 2.3 g/L. The cells were incubated in duplicate cultures with various concentrations of the drugs for 30 min. Then 10 mCi of [^{3}H]uridine was added to label the RNA synthesized during a 30 min incubation at 37 °C. The labeled RNA was isolated by the rapid procedure of Chomczynski and Sacchi (1987). This involves homogenization of the cells in the presence of guanidine thiocyanate to inhibit RNases, acid phenol/chloroform extraction to remove protein and DNA, concentration by isopropanol precipitation, and dissolving the RNA in TE (10 mM Tris-HCl, pH 8.0, 1 mM EDTA). The label incorporated into RNA was determined by liquid scintillation counting.

RESULTS AND DISCUSSION

Synthesis

AMD analogues in which *N*-methyl-L-valine residues were replaced with L- and D-forms of *N*-methylvalines (L-Val-AMD, D-Val-AMD), *N*-methylthreonines (L-Thr-AMD, D-Thr-AMD), *N*-methylphenylalanines (L-Phe-AMD, D-Phe-AMD), *N*-methyltyrosines (L-Tyr-AMD, D-Tyr-AMD), and *N*-methyl-*O*-methyltyrosines (L-OMT-AMD, D-OMT-AMD) have been synthesized by a slightly modified procedure of Mauger *et al.* (1991). The molecular formulas of AMD and AMD analogues are illustrated in Figure 1. L-Val-AMD is AMD itself, while the others are new compounds. A schematic synthetic procedure is shown in Scheme 1.

Molecular Modeling

A simple molecular modeling study has been carried out using the crystal structure of the $d(GAAGCTTC)_2$−AMD complex (Shinomiya *et al.*, 1995). The L-Phe-AMD and D-Phe-AMD molecules were built by replacing the *N*-methyl-L-valine residues of the AMD molecule with *N*-methyl-L-phenylalanine and *N*-methyl-D-phenylalanine residues, respectively. The model crystal structures were refined by the program X-PLOR (Brünger, 1993). In the calculation, the weight (W_A) for the X-ray contribution part was set to very small number (1.0) so that the energies of the molecular geometry and interaction were minimized. The water molecules found in the crystal structure (Shinomiya *et al.*, 1995) were included in the calculations. The structures were refined by 500 cycles of POSITIONAL protocol of X-PLOR. The total energies of the model systems were convergent at −1063 kcal/mol for L-Phe-AMD, −1068 kcal/mol for D-Phe-AMD, and −1043 kcal/mol for AMD itself. The refined complex structures are illustrated in Figure 2. Although the model structures may not represent the actual DNA−drug complex structures, they should suggest how the substituted bulky aromatic groups affect the complexes.

As discussed in the crystal structure papers (Kamitori & Takusagawa, 1992; Shinomiya *et al.*, 1995), the DNA was unwound asymmetrically by intercalation of the AMD molecule into the middle GC sequence. This asymmetric unwinding of the DNA helix creates differently shaped minor grooves above and below the intercalation site. One is a relatively wide and shallow groove, and the other is a relatively narrow and deep groove. The cyclic depsipeptide

Scheme 1: Syntheses of AMD Analogues[a]

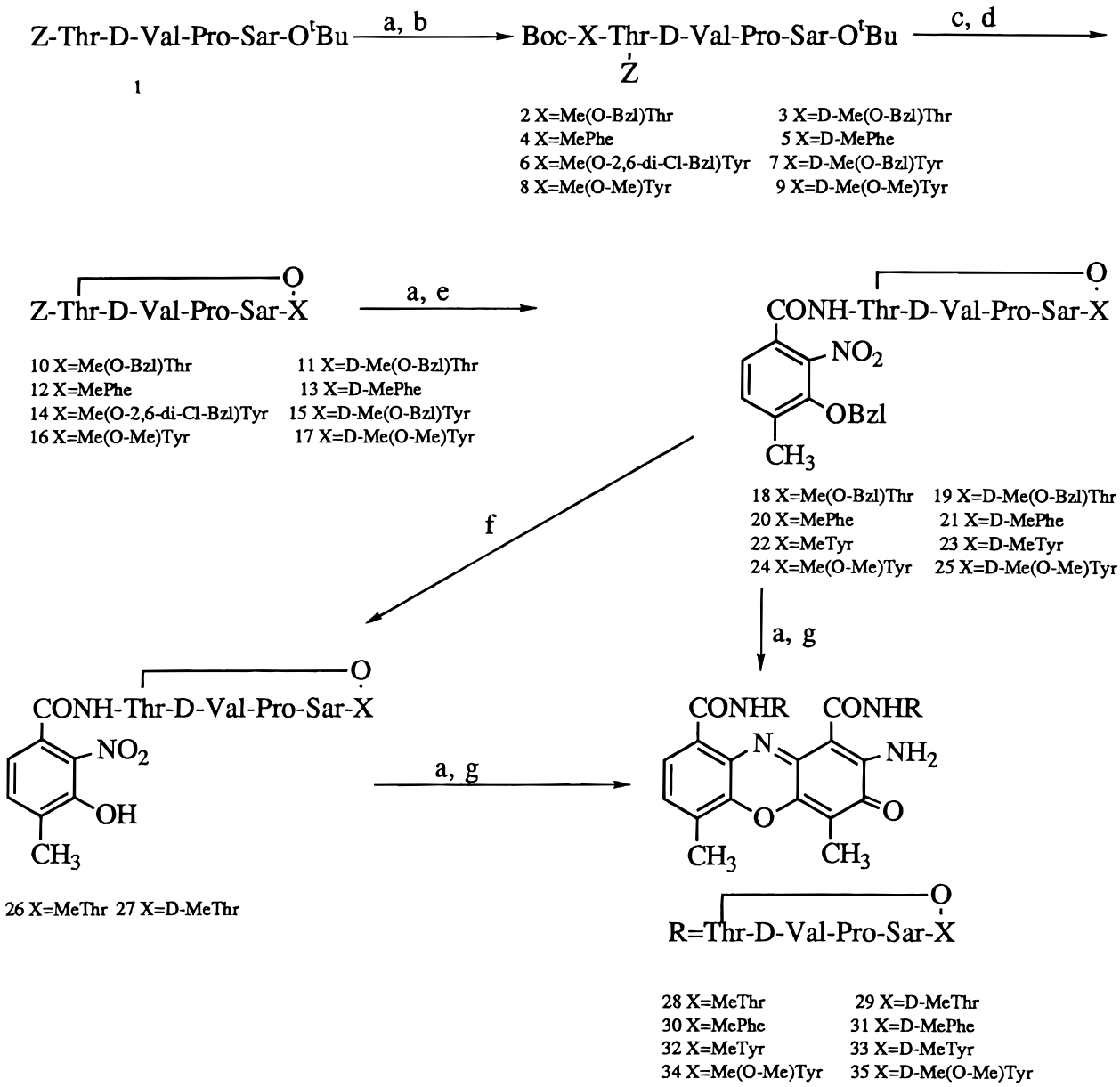

(a) Pd/C, H_2; (b) Boc-X-OH, DCC, DMAP; (c) F_3C-COOH; (d) Bop-Cl, $N(Et)_3$;
(e) 3-Benzyloxy-4-methyl-2-nitrobenzoic acid, DCC; (f) F_3C-SO_3H
(g) $K_3Fe(CN)_6$, PH=7.12

[a] The product numbers 1−35 correspond to the product numbers in the supporting information.

α-ring attached to C9 of the chromophore fits quit well into the wide and shallow groove, whereas the β-ring attached to the C1 of the chromophore does not fit well into the narrow and deep groove and appears to be forced out of the DNA minor groove. As a result, there is a large space between the *N*-methyl-L-valine residue and the AT base pair adjacent to the intercalation site. As described in the previous paper (Shinomiya *et al.*, 1995), the isopropyl group of the *N*-methyl-D-valine fits well into this space. In the D-Phe-AMD analogue model, even the bulky phenyl group attached to the β-ring fits well into the minor groove space, whereas the phenyl group attached to the α-ring is apparently forced out of the minor groove since the α-ring already fills the minor groove, leaving too little space for the bulky phenyl group. As will be discussed below, the weaker DNA associations of the D-aromatic analogues might be due to this steric hindrance of the substituted aromatic groups at the α-ring, but not the β-ring. In conclusion, this molecular modeling study indicates that the D-form analogues can bind intercalatively at the GC site as AMD does. The amino acid side chain at the β-ring might enhance the association with DNA, whereas the amino acid side chain at the α-ring might inhibit the DNA binding of the analogues.

For the L-Phe-AMD analogue model, the substituted phenyl groups apparently do not inhibit the interaction between the cyclic depsipeptides and the DNA minor groove

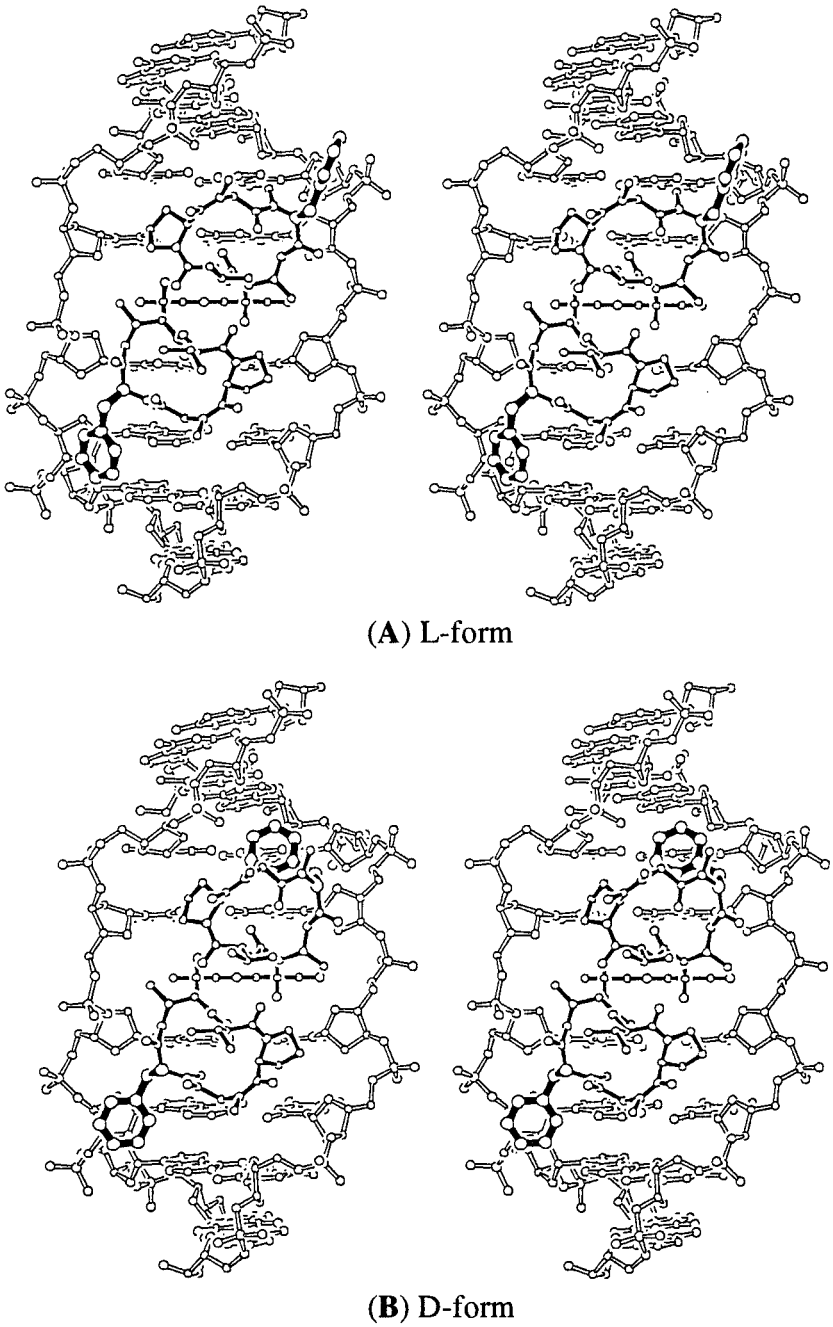

FIGURE 2: DNA−(Phe-AMD) complex models derived from the crystal structure of d(GAAGCTTC)$_2$−AMD. The *N*-methyl-L-valine residues were replaced with *N*-methyl-L-phenylalanine residues (A) and *N*-methyl-D-phenylalanine residues (B). The model structures were refined 500 cycles by X-PLOR using the positional refinement protocol. The weight (W_A) for the X-ray contribution part was set to 1.0. The DNA and drug are drawn with open and solid bonds, respectively. The substituted phenyl groups are drawn with thick solid bonds.

surfaces. The phenyl group attached to the α-ring might be able to interact with the minor groove. In particular, if the valine residue is replaced with a tyrosine residue, the phenol OH will be able to form a hydrogen bond with the O2 carbonyl oxygen of cytosine or thymine bases. As will be described below, this hydrogen bond formation might greatly increase the association constant of the L-Tyr-AMD analogue.

Consideration of DNA Binding Experiment

From the crystal structures of AMD and AMD analogues (Kamitori & Takusagawa 1992, 1994; Shinomiya *et al.*, 1995), it is very clear that the chromophore of AMD cannot bind to the major and/or minor groove of DNA as do typical minor groove binding agents, such as netropsin and distamycin (Dickerson *et al.*, 1986), since there are not enough polar groups (−NH, −OH, >N, =O, and >O) on the surface of the chromophore. Therefore, the binding mode available to the AMD analogues is either intercalation or weak side-binding to the charged phosphate backbone of DNA. Since the visible spectrum (350−600 nm) of the chromophore is slightly shifted to the longer wavelength region (red shift) and the magnitude of absorbance is reduced (hypochromic effect) by the drug intercalating into the nucleic acid, the binding characteristics of the AMD analogues can be observed in the spectra of the analogues by titration of DNA solution. The following five self-complementary 16-mer oligonucleotides were utilized to examine the binding characteristics of AMD and AMD analogues.

DNA-1: d(T-A-T-A-T-A-**T-G-C-A**-T-A-T-A-T-A)

DNA-2: d(T-A-T-A-T-A-**C-G-C-G**-T-A-T-A-T-A)

DNA-3: d(A-T-A-T-A-T-**A-G-C-T**-A-T-A-T-A-T)

DNA-4: d(A-T-A-T-A-T-**G-G-C-C**-A-T-A-T-A-T)

DNA-0: d(T-A-T-A-T-A-T-A-T-A-T-A-T-A-T-A)

These oligonucleotides were selected for the following reasons:

(1) AMD and its analogues can intercalate only at GC in -XGCY- sequences. DNA-1, -2, -3, and -4 have only GC in the middle of the sequence. Thus, the visible spectra of AMD analogues titrated by DNAs can be interpreted relatively simply.

(2) AMD and its analogues should interact with the DNA residues adjacent to the intercalation site. Thus, all four possible symmetrical sequences (-TGCA-, -CGCG-, -AGCT-, -GGCC-) were used.

(3) Purine−pyrimidine alternating sequences form a stable double-stranded helix even at a relatively low concentration (~0.2 μM). A DNA melting experiment indicates that these five oligonucleotides indeed form double-stranded helices under 10 °C (Figure 3).

(4) Since DNA-0 does not have an AMD intercalation site (-GC-), the interactions of this DNA with the AMD analogues should occur only through side-binding. Thus, the side-binding effects on the spectra obtained with DNA-1, -2, -3, and -4 can be estimated by comparison with the spectra obtained with DNA-0.

Although the binding experiment was carried out at a relatively low drug concentration (1.0 μM) in order to eliminate any possibility of dimerization of the drug in an aqueous solution, the possibility of dimerization in the buffer solution used in this study was examined by measuring the absorbance at 440 nm at various temperatures (20, 30, 40, 50, 60, and 70 °C). No significant change in the absorbance was observed, suggesting that neither AMD nor AMD analogues formed detectable amounts of dimers at 1 μM concentration. The dimerization equilibrium constant of AMD was reported to be 2.7×10^3 M^{-1}, as determined by the NMR method (Angerman *et al.*, 1972). Using this dimerization equilibrium constant, 99.7% of AMD molecules are calculated to be in monomer form at 1 μM concentration. The dimerization equilibrium constants of the AMD analogues might be slightly larger than the value of AMD, since the substituted aromatic amino acid residues can stabilize the dimer formation by stacking on the chromophore as seen in the crystal structure of 2,2′-D-*O*-methyltyrosine AMD (Chu *et al.*, 1994). However, even if the dimerization equilibrium constants of AMD analogues are estimated to be 2 orders of magnitude higher than the value for AMD, the equilibrium calculation indicates that 81.9% of the molecules are in monomer form at 1 μM concentration.

Overall DNA Binding Characteristics of AMD Analogues

The visible absorption spectra of AMD analogues were measured with seven different concentrations of DNA-0, and the representative spectra of AMD and Tyr-AMD analogues are shown in Figure 4. As expected, the spectra were not shifted by titration of the DNA, indicating no intercalation.

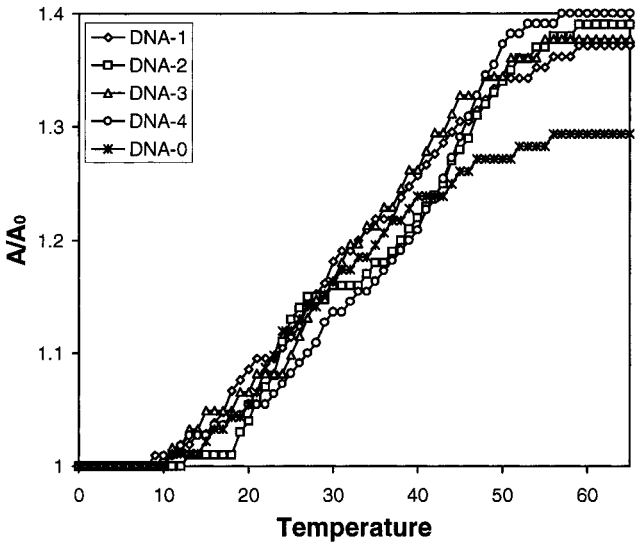

FIGURE 3: Melting profiles of DNA-1, DNA-2, DNA-3, DNA-4, and DNA-0. The concentrations of DNAs are 0.2 μM.

However, significant hypochromic effects were observed. The D-aromatic analogues showed relatively large hypochromic effects, whereas the L-aliphatic analogues showed small effects. These hypochromic effects should be caused by weak side-bindings of analogues. The magnitudes of the spectrum changes are well correlated with the amount of the titrated DNA, suggesting that the hypochromic effect is a linear function of [DNA]/[drug]. Thus, an absorption spectrum $A_r(\lambda)$ of r = [DNA]/[drug] was approximated as

$$A_r(\lambda) = (1 - C_2 r)A_0(\lambda)$$

The coefficient C_2 of the hypochromic effect was determined by a least-squares fitting and was found to be 0.020 for L-aliphatic analogues, 0.043 for D-aliphatic analogues, 0.079 for L-aromatic analogues, and 0.117 for D-aromatic analogues. As will be described below, the C_2 values were used for the association constant calculation.

The visible absorption spectra of AMD analogues were measured at seven different concentrations of the oligonucleotides. The spectra of the aliphatic analogues (Val and Thr) are quite similar to each other, and the spectra of the aromatic analogues (Phe, Tyr, and OMT) are also quite similar to each other. Thus the spectra of Val and Tyr analogues are shown in Figure 4. The spectra of both L- and D-form analogues titrated by DNA-1, DNA-2, and DNA-3 show significant red shifts as well as hypochromic effects, indicating that the AMD analogues bind intercalatively to -XGCY- sites of the DNAs. However, the spectra titrated by DNA-4 did not show significant red shifts, indicating that the AMD analogues bind only weakly to this DNA.

The spectra were analyzed numerically by a slightly modified method described in our previous paper (Chu *et al.*, 1994). The coefficients C_0 and C_1 and $\Delta\lambda$ in eq 1 were determined by minimizing $\sum[A_c(\lambda)_{obsd} - A_c(\lambda)_{calcd}]^2$.

$$A_c(\lambda)_{calcd} = C_0 A_d(\lambda)_{obsd} + C_1 A_d(\lambda - \Delta\lambda)_{obsd} \qquad (1)$$

where $A_c(\lambda)_{calcd}$ and $A_d(\lambda)_{obsd}$ are calculated complex absorbance and observed drug absorbance at wavelength λ. $\Delta\lambda$ is the red shift of spectra by drug intercalation. The association constant (k) and hypochromic effect (H) were

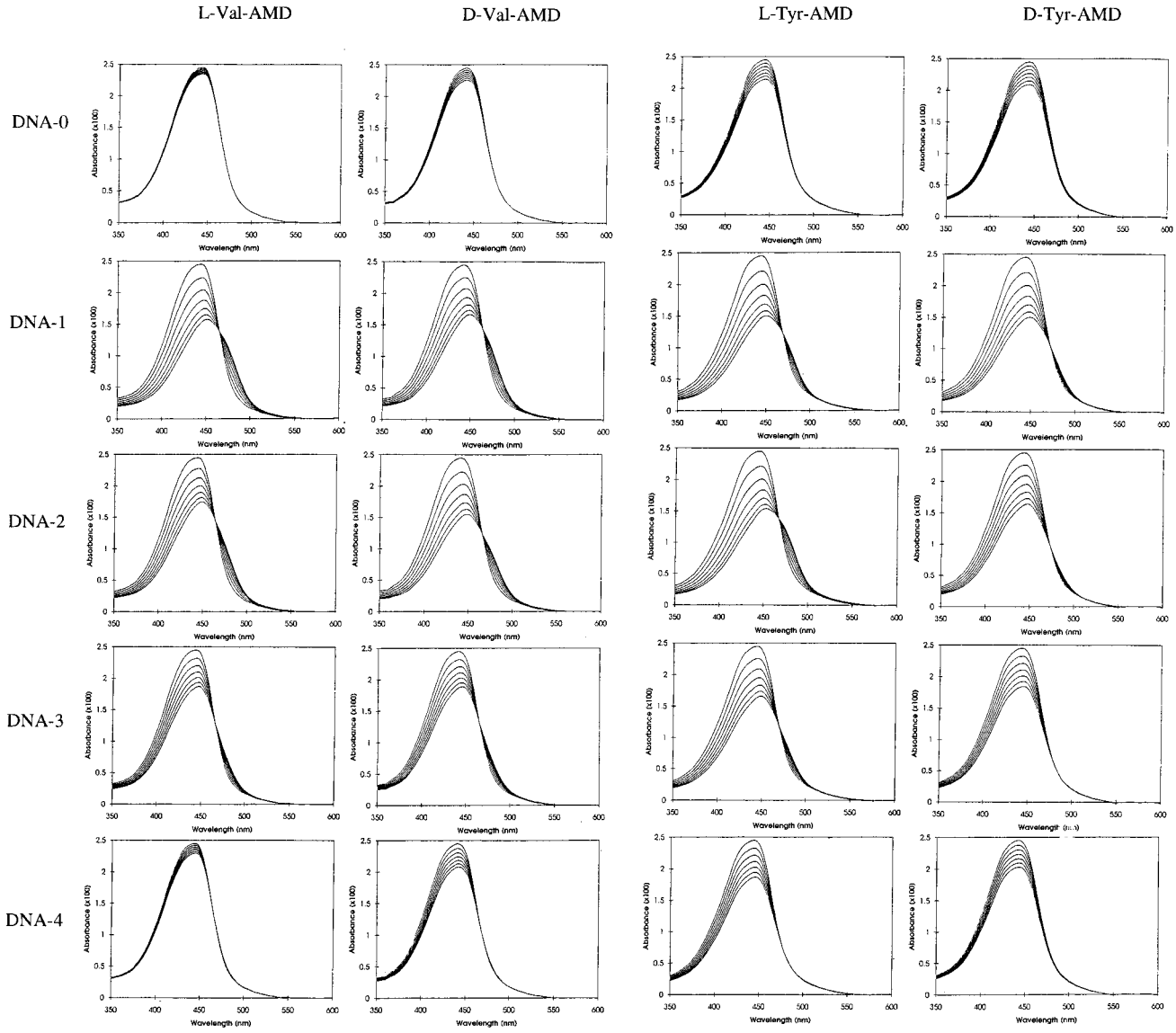

FIGURE 4: (Left two columns) Visible absorption spectra of L-Val-AMD and D-Val-AMD titrated by DNA-0, DNA-1, DNA-2, DNA-3, and DNA-4. The drug concentration is scaled to 1.0 μM. The ratios of [DNA]/[drug] are 0.0, 0.2, 0.4, 0.6, 0.8, 1.0, and 1.2, respectively. The spectra of the drug and each DNA titration are drawn from top to bottom, respectively. (Right two columns) Visible absorption spectra of L-Tyr-AMD and D-Tyr-AMD titrated by DNA-0, DNA-1, DNA-2, DNA-3, and DNA-4. The drug concentration and titration conditions are the same as in the left two columns.

calculated from the coefficients C_0 and C_1 as shown below.

$$k = \alpha/[(1 - \alpha)(r - \alpha)D] \quad \text{and} \quad H = C_1/\alpha$$

where $\alpha = (1 - C_0 - C_2 r)/(1 - C_2 r)$, and r and D are the ratio of DNA per drug and drug concentration, respectively. C_2 is a coefficient of the hypochromic effect of side-binding obtained from the spectra obtained with DNA-0. Although we assumed $C_0 = 1 - \alpha$ in the previous paper (Chu *et al.*, 1994), we modified it to $C_0 = 1 - \alpha - C_2 r(1 - \alpha)$, since we have obtained side-binding effects (coefficient C_2) from the titration of DNA-0 as described above. The association constant (k), hypochromic effect (H), and red shift ($\Delta\lambda$) obtained from the spectra are listed in Table 1. The red shifts of the spectra are constantly around 22 nm. On the other hand, there is a trend in the hypochromic effects in spite of the correction for side-binding. The hypochromic effects of aliphatic analogues (Val and Thr) are slightly smaller than those of aromatic analogues (Phe, Tyr, and OMT).

The L-Val (AMD) and L-Thr aliphatic analogues have clear sequence specificity, *i.e.*, TGCA > CGCG > AGCT > GGCC. Our result agrees with Chen's observation of AMD binding strength (Chen, 1988, 1992). Although the binding preference order of the L-aromatic analogues is similar to that of the aliphatic analogues, there is no significant reduction in binding affinity between TGCA and CGCG. With the L-Tyr analogue, the binding affinities to the TGCA and CGCG sequences are inverse, *i.e.*, CGCG > TGCA > AGCT > GGCC. For the D-form analogues, the binding order is the same as that of the L-aliphatic analogues. Both L- and D-analogues bind very little to -GGCC- sequence, especially the L-aliphatic and D-aromatic analogues, which show no detectable binding. It is quite clear that AMD analogues bind preferably to pyrimidine−purine alternating sequences. Thus, the binding preference might be due to the different DNA helical conformations. As discussed in the molecular modeling study, d(GA**AGCT**TC) is unwound asymmetrically at the intercalation site, and, for this reason, the β-ring does not fit well into the minor groove. Similar asymmetrical unwinding might be further amplified in the GGCC sequence site, and, as a result, the cyclic depsipeptide

Table 1: Association Constants ($k \times 10^{-6}$ M^{-1}), Hypochromic Effect (H), Red Shift ($\Delta\lambda$), and Complex Formation (%) at Both Drug and DNA Concentrations of 100 nM

	L-form				D-form			
analogue	*k*	*H*	$\Delta\lambda$	complex	*k*	*H*	$\Delta\lambda$	complex
DNA-1								
Val	5.0	0.57	23	27	3.7	0.60	21	22
Thr	3.9	0.57	22	23	2.3	0.60	22	16
Phe	4.3	0.53	22	25	2.3	0.49	20	16
Tyr	4.0	0.53	20	23	2.2	0.49	20	16
OMT	3.3	0.47	21	21	1.0	0.46	16	8
DNA-2								
Val	2.4	0.60	22	17	3.0	0.52	24	20
Thr	2.0	0.57	22	15	1.4	0.59	22	11
Phe	3.2	0.59	22	20	0.7	0.49	16	6
Tyr	5.4	0.58	22	28	0.9	0.48	22	8
OMT	2.4	0.53	22	17	0.9	0.40	21	8
DNA-3								
Val	0.9	0.54	22	8	0.8	0.58	22	7
Thr	0.7	0.63	25	7	0.5	0.63	23	5
Phe	1.0	0.46	24	8	0.2	0.40	23	2
Tyr	1.4	0.53	22	11	0.3	0.47	18	3
OMT	0.8	0.41	22	7	0.2	0.44	13	2
DNA-4								
Val	0.1	0.66	17	1	0.3	0.56	15	3
Thr	0.1	0.67	24	1	0.1	0.70	22	1
Phe	0.2	0.43	22	1	–	–	0	–
Tyr	0.4	0.47	17	3	–	–	0	–
OMT	0.3	0.35	19	3	–	–	0	–

would not fit into the minor groove. This could be the reason that AMD analogues bind very poorly to the -GGCC- sequence.

These association constants indicate that the modifications of the *N*-methyl-L-valine residues in the AMD molecule do affect the DNA binding characteristics of the analogues. The L-aromatic analogues (Phe, Tyr, OMT) bind slightly better than the L-aliphatic analogues (Val and Thr) except for DNA-1 (-TGCA-), whereas the D-aliphatic analogues bind constantly better than the D-aromatic analogues. In the L-form analogues, the L-Tyr analogue has the highest overall association constant, whereas the D-Val analogue has the highest association constant among the D-form analogues.

Binding Characteristics of D-Form Analogues

Although the molecular modeling study described above predicts that the D-form analogues can bind intercalatively into DNA as strongly as the L-form analogues, we were interested in examining how the DNA binding characteristics are changed by introducing the D-form amino acid residues into the L-amino acid residue sites of the natural antibiotic AMD. As described above, the overall DNA binding capacity of the D-form analogues are decreased. However, the D-aliphatic analogues (Val and Thr) bind the DNAs as strongly as the L-aliphatic analogues. Interestingly, the D-Val substitution increases the DNA binding capacity of the analogue to CGCG and GGCC sites over the natural L-Val compound (AMD itself). On the other hand, the D-aromatic analogues bind well only to the DNA-1 (TGCA). There are significant reductions in their binding capacities with other DNAs. These binding characteristics indicate that the substitution of the D-aromatic residues creates a unique four-base sequence preference (TGCA). The sequence selectivity could be due to the following three causes.

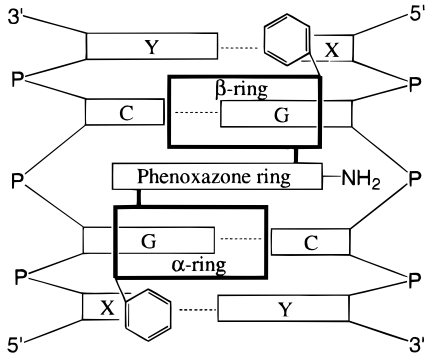

FIGURE 5: Schematic diagram of the D-Phe-AMD binding site. The substituted phenyl groups are located near the bases X. The cyclic depsipeptide attached at C9 of the chromophore is called the α-ring, and the other cyclic depsipeptide, which is attached at C1 and is near the amino group (NH_2), is called the β-ring (Meienhofer & Atherton, 1977).

(1) As schematically illustrated in Figure 5, the aromatic groups of the D-amino acid residues should locate near the X base (T for DNA-1, C for DNA-2, A for DNA-3, and G for DNA-4). The pyrimidine bases (T and C) are smaller than the purine bases (A and G). Thus, X = T or C gives a slightly larger space for the substituted aromatic group.

(2) The minor groove surface of the G-C base pair is quite hydrophilic, and thus the [G]-N2-H_2···O2-[C] should be hydrated, whereas the [A]···O2-[T] is not as hydrophilic as the [G]-N2-H_2···O2-[C]. Thus, the hydrophobic phenyl group can interact more easily with the A-T base pair than with the G-C base pair.

(3) The L-form analogues indicate that the cyclic depsipeptide rings of the AMD analogues fit better into the minor groove of the pyrimidine−purine alternating sequences 5′-TGCA-3′ and 5′-CGCG-3′ than into the minor groove of the nonalternating sequences 5′-AGCT-3′ and 5′-GGCC-3′.

The DNA binding data suggest that if the phenyl group is slightly modified to increase its T-base affinity and to

Table 2: Solubility (μg/mL) in Aqueous Solution at 22 ± 1 °C, Drug Concentrations (nM) at 50% Inhibition of RNA Synthesis (IC_{50}) in HeLa Cells, and the Calculated Bound Drug Concentrations (nM) at 100 nM Drug and XGCY Binding Site Concentrations *in vitro*

	L-form			D-form		
drug	solubility	IC_{50}	bound drug	solubility	IC_{50}	bound drug
Val	2900	30	52	160	1	52
Thr	4700	>1000	45	180	100	33
Phe	20	10	55	30	20	25
Tyr	40	80	66	40	80	26
OMT	10	8	47	30	80	20

decrease its affinity for other bases, such an analogue binds only at the 5′-TGCA-3′ sequence.

Water-Solubilities of AMD Analogues

Solubilities of the analogues in water were determined, since this physical character may play an important role in their binding and biological characteristics. As listed in Table 2, the solubilities of the aromatic analogues are very low in comparison with L-Val (AMD). Surprisingly, the water solubility of D-Val and D-Thr is also quite low in comparison with L-Val and L-Thr. As discussed in our previous paper (Chu *et al.*, 1994), the water solubilities of the analogues are very peculiar and are almost impossible to predict. For example, the water solubility of 2,2′-D-Thr-AMD is only 31 μg/mL while that of 2,2′-D-Val-AMD is 2900 μg/mL (Chu *et al.*, 1994). However, the differences between 2,2′-D-Val-AMD and 2,2′-D-Thr-AMD [-$CH(CH_3)_2$ *vs* -$CH(OH)CH_3$] are slight even though the -$CH(OH)CH_3$ group is generally more hydrophilic than the -$CH(CH_3)_2$ group. In contrast to 2,2′-D-Thr-AMD, the L-Thr analogue is much more water soluble (4700 μg/mL) than AMD. These data indicate that the hydration environments play an important role in the water solubility of the analogues. In connection with this observation, the binding of AMD is often described as being entropically driven in terms of the solvation of the free drug (Gellert *et al.*, 1965; Marky *et al.*, 1983). The hydration environments of the AMD analogues should be drastically changed by introducing different amino acid residues in the cyclic depsipeptides. It is noted that AMD is the only compound that has hydrophobic amino acid residues at the 2- and 5-positions of the cyclic depsipeptides but still has a relatively high water solubility.

RNA Polymerase Inhibitory Activities

The RNA polymerase inhibitory activities of the AMD analogues *in vivo* have been examined using human cells (HeLa). The drug concentrations at 50% inhibition level (IC_{50}) are listed in Table 2. All AMD analogues except for L-Thr-AMD severely inhibit RNA synthesis at relatively low drug concentrations (<100 nM). It should be noted that the D-Val, L-OMT, L-Phe, and D-Phe analogues inhibit RNA synthesis more strongly than AMD itself. In order to interpret the inhibitory data in terms of the DNA binding capacity, the concentrations of the bound drugs were calculated at 100 nM drug and DNA binding site. Since the cells are in a large pool of the drug solution at constant concentration, the amount of a bound drug can be a sum of the individual bound drug concentrations. When the L-Thr analogue is excluded, the DNA binding capacities and the RNA synthesis inhibitory activities (IC_{50}) of the AMD analogues are approximately on the same level. The presence of a hydrophilic group on the surface of an analogue might reduce the diffusion capacity of the analogue into cells, and consequently, the biological activities of the analogue are reduced. Apparently the L-Thr analogues cannot diffuse well into cells, and this makes it inactive in RNA synthesis inhibition. This is consistent with the relatively high water solubility of this compound. Interestingly, however, the L-Tyr, D-Thr, and D-Tyr analogues, which have relatively low water solubility, are quite active, indicating that those analogues can diffuse into cells. Thus, a molecular shape is an important diffusing factor. In general, the DNA binding capacities of the D-form analogues are slightly weaker than the L-form analogues, and consequently the RNA synthesis inhibitory activities are slightly lower than the L-form analogues. However, it should be noted that the D-Val analogue binds DNA at the same level as the L-Val (AMD itself) and inhibits the RNA synthesis much more strongly than AMD (30-fold improvement). Also, the RNA synthesis inhibitory activities of the L-Phe, L-OMT, and D-Phe analogues are better than that of the parent AMD.

ACKNOWLEDGMENT

We thank Mrs. Judy Bevan for technical help with the transcription inhibition experiments.

SUPPORTING INFORMATION AVAILABLE

The details of synthetic procedures of L-Thr, L-Phe, L-Tyr, L-OMT, D-Val, D-Thr, D-Phe, D-Tyr, and D-OMT analogues are given (9 pages). Ordering information is given on any current masthead page.

REFERENCES

Angerman, N. S., Victor, T. A., Bell, C. L., & Danyluk, S. S. (1972) *Biochemistry 11*, 2402−2411.
Bailey, S. A., Graves, D. E., Rill, R., & Marsch, G. (1993) *Biochemistry 32*, 5881−5887.
Breslauer, K. J., Remeta, D. P., Chou, W.-Y., Rerrante, R., Curry, J., Zaunczkoski, D., Snyder, J. G., & Marky, L. A. (1987) *Proc. Natl. Acad. Sci. U.S.A.* 84, 8922−8926.
Brockmann, H., & Lackner, H. (1968) *Chem. Ber. 101* 1312.
Brown, S. C., Mullis, K., Levenson, C., & Shafer, R. H. (1984) *Biochemistry 23*, 403−408.
Brünger, A. T. (1993) *X-PLOR 3.1. A System for X-ray Crystallography and NMR*, Yale University Press, New Heaven, CT.
Cantor, C. R., & Warshaw, M. M. (1970) *Biopolymers 9*, 1059−1077.
Chen, F.-M. (1992) *Biochemistry 31*, 6223−6228.
Chen, F.-M. (1988) *Biochemistry 27*, 6393−6397.
Chomczynski, P., & Sacchi, N. (1987) *Anal. Biochem. 162*, 156.
Chou, W. Y., Marky, L. A., Zaunczkowski, D., & Breslauer, K. J. (1987) *J. Biomol. Struct. Dyn. 5*, 345−359.
Chu, W., Kamitori, S., Shinomiya, M., Carlson, R. G., & Takusagawa, F. (1994) *J. Am. Chem. Soc. 116*, 2243−2253.
Dickerson, R. E., Kopka, M. L., & Pjura, P. (1986) *Chem. Scr. 26B*, 139−145.
Farber, S. J. (1966) *J. Am. Med. Assoc. 198*, 826−836.

Gellert, M., Smith, C. E., Neville, D., & Felsenfeld, G. (1965) *J. Mol. Biol. 11*, 445−457.
Goldberg, J. H., & Friedman, P. A. (1971) *Annu. Rev. Biochem. 40*, 775−810.
Goodismen, J., Rehfuss, R., Ward, B., & Dabrowiak, J. C. (1992) *Biochemistry 31*, 1046−1058.
Kamitori, S., & Takusagawa, F. (1992) *J. Mol. Biol. 225*, 445−456.
Kamitori, S., & Takusagawa, F. (1994) *J. Am. Chem. Soc. 116*, 4154−4165.
Kersten, H., & Kersten, W. (1974) Actinomycin, in *Inhibitors of Nucleic Acid Synthesis*, pp 40−66, Springer Verlag, Berlin.
Lewis, J. L. (1972) *Cancer 30*, 1517−1521.
Liu, X., Chen, H., & Patel, D. J. (1991) *J. Biomol. NMR 1* 323−347.
Marina, N., Fontanesi, J., Kun, L., Rao, B., Jenkins, J. J., Thompson, E. I., & Etcubanas, E. (1992) *Cancer 70*, 2568−2575.
Marky, L. A., Snyder, J. G., Remeta, D. P., & Breslauer, K. (1983) *J. Biomol. Struct. Dyn. 1*, 487−507.
Mauger, A. B. (1980) The Actinomycins, in *Topics in Antibiotic Chemistry* (Sammes, P. G., Ed.) pp 224−306, E. Horwood, Chichester.
Mauger, A. B. (1990) Actinomycins, in *The Chemistry of Antitumor Agents* (Wilman, E. V., Ed.) pp 403−409, Blackie & Son, Glasgow.
Mauger, A. B., Stuart, O. A., & Katz, E. (1991) *J. Med. Chem. 34*, 1297−1301.
Meienhofer, J., & Atherton, E. (1977) Structure−activity relationships in the actinomycins, in *Structure−Activity Relationships among the Semisynthetic Antibiotics* (Perlman, D., Ed.) pp 427−529, Academic Press, New York.
Müller, M., & Crothers, D. M. (1968) *J. Mol. Biol. 35*, 251−290.
Nakamura, E., Kaneko, Y., Takenawa, J., & Sasaki, M. (1992) *Acta Urol. Jpn. 38*, 913−918.
Newlands, E. S., Bagshawe, K. D., Begent, R. H. J., Rustin, G. J. S., & Holden, L. (1991) *Br. J. Obstet. Gynaecol. 98*, 550−557.
Phillips, D. R., & Crothers, D. M. (1986) *Biochemistry* 25, 7355−7362.
Scamrov, A. V., & Beabealashvilli, R. Sh. (1983) *FEBS Lett. 164*, 97−101.
Schink, J. C., Singh, D. K., Rademaker, A. W., Miller, D. S., & Lurain, J. R. (1992) *Obstet. Gynecol. (N.Y.) 80*, 817−820.
Shinomiya, M., Chu, W., Carlson, R. G., Weaver, R. F., & Takusagawa, F. (1995). *Biochemistry 34*, 8481−8491.
Snyder, J. G., Hartman, N. G., D'Estantoit, B. L., Kennard, O., Remeta, D. P., & Breslauer, K. J. (1989) *Proc. Natl. Acad. Sci. U.S.A. 86*, 3968−3972.
Sobell, H. M., Jain, S. C., Sakore, T. D., & Nordman, C. E. (1971) *Nature, New Biol. 231*, 200−205.
Takusagawa, F. (1985) *J. Antibiotics 38*, 1596−1604.
Takusagawa, F., Dabrow, M., Neidle, S., & Berman, H. M. (1982) *Nature 296*, 466−469.
Waring, M. (1981) Inhibitors of nucleic acid synthesis, in *The Molecular Basis of Antibiotics Action* (Gale, F., *et al.*, Eds.) pp 258−401, Wiley, London.
Zhou, N., James, T. L., & Shafer, R. H. (1989) *Biochemistry 28*, 5231−5239.

BI960828R